Imperial College London
Department of Physics
Theoretical Physics Group

On the Black Hole Information Paradox and the Page Curve

Author: Imran Abdul Rahman

Supervisor: Prof. Toby Wiseman

Submitted in part fulfilment of the requirements for the degree of
Master of Science of Imperial College London

Abstract

In this review, we summarise recent developments in the black hole information paradox, specifically focusing on the Page curve. We first provide an exposition of the paradox with the nice slice argument. We then explain how theories such as the AdS/CFT correspondence can shed light on the paradox. Finally, we introduce the Page curve before reviewing recent progress in reproducing it.

Acknowledgements

I would like to thank Prof. Toby Wiseman for his supportive supervision and infinite patience in answering my questions. In addition, many thanks to my family for supporting me as always, and to my friends for putting up with my nonsense.

Contents

Chapter 1

Introduction

1.1 A brief history

Black holes are fascinating objects. Soon after Albert Einstein announced his theory of general relativity in 1915, Karl Schwarzschild found his eponymous, spherically symmetric solution which admitted the tantalising possibility of black holes, which has become an active area of research ever since. It was only recently in 2019 when the first image of a black hole was released following observations by the Event Horizon Telescope.

Besides its defining property of being a region from which no causal observer can escape from, it also obeys the no-hair theorem, which states that all black holes can be completely characterised by its mass, charge and angular momentum. This already provided a bit of a problem, since it implied that the information of whatever fell into a black hole would not be able to be distinguished from outside the event horizon. Simply put, the result from an elephant falling into a black hole would look the same as if it were instead an identical massive boulder.

This provided some consternation, but it was speculated that this information would be hidden behind the horizon. But in 1975, Stephen Hawking discovered that black holes emit the characteristic radiation that still bears his name [1]. We can roughly think of Hawking radiation involving the creation of an entangled pair of particles near the horizon, where one particle

escapes whereas the other falls into the black hole. The main implication is that all black holes will gradually evaporate and eventually disappear. This means that either information is truly lost in black holes, or that information has been preserved by Hawking radiation by some mechanism.

In 1997, a public wager was announced between John Preskill on one side, and Hawking and Kip Thorne on the other. Preskill contended that unitarity is preserved and information is not lost in black holes. On the other hand, Hawking and Thorne believed that information is indeed lost in black holes. Hawking has since conceded the bet to Preskill, although Thorne has not followed suit.

A key tenet of black holes is that an observer passing freely through the horizon does not experience anything strange. But some resolutions to the paradox posit that a traditional black hole event horizon does not form and so some drama is encountered at the horizon. One resolution is the concept of a firewall, which purports that high energy particles are encountered at the horizon [2, p. 3]. Another is that black holes are 'fuzzballs', which has the corollary of doing away with the concept of a black hole interior entirely. But there are difficulties with both hypotheses, and it is argued in [3, p. 117] that resorting to firewalls or fuzzballs are not necessary to solve the information paradox for evaporating black holes.

1.2 Black hole preliminaries

As mentioned in the previous section, Hawking showed in his landmark paper how black holes emit radiation by considering quantum field theory in a Schwarzschild spacetime [1]. A modern rederivation of Hawking radiation can be found in [3, p. 8-13]. In addition, Hawking showed that this radiation obeyed a thermal spectrum with the characteristic Hawking temperature T_H given by

$$T_H = \frac{\hbar\kappa}{2\pi k_B}, \tag{1.1}$$

where κ is the surface gravity of the black hole [4, p. 380].

Not only do black holes have a temperature, they also can be thought of possessing entropy. Prior to the discovery of Hawking radiation, Bekenstein posited that the entropy of a black hole is directly proportional to its area, although he did not manage to completely determine the constant of proportionality. But Hawking managed to fix this constant of proportionality from his derivation of (1.1), and so the formula for the entropy of a black hole (known as the Bekenstein-Hawking formula) is given by

$$S_{BH} = \frac{k_B A}{4l_P^2} = \frac{k_B c^3 A}{4G_N \hbar}, \tag{1.2}$$

where $l_P = \sqrt{\frac{G_N \hbar}{c^3}}$ is the Planck length.

Now as a black hole emits Hawking radiation and gradually evaporates, it loses mass and so the area of the event horizon shrinks. From (1.2), it would naively seem that the entropy will decrease over time. But the total entropy for a black hole and its surroundings has a contribution from quantum fields outside the horizon. This total entropy is known as the 'generalised' entropy, which we can write as

$$S = S_{BH} + S_{\text{outside}}, \tag{1.3}$$

where S_{outside} denotes the entropy of matter outside the horizon of the black hole [5, p. 5].

1.3 Fine and coarse-grained entropy

When a black hole emits Hawking radiation, the particles that escaped are entangled with the ones that fell into the black hole. There exists an entropy associated with entanglement, which is von Neumann entropy. Given a state with corresponding density matrix ρ, the von Neumann entropy S_{vN} is given by [6]

$$S_{vN} = -\text{tr}(\rho \ln \rho). \tag{1.4}$$

Now, we can decompose the density matrix as $\rho = \sum_i \lambda_i |i\rangle\langle i|$, where λ_i denotes the set of eigenvalues of ρ. Using this form, we can express the S in the more useful form

$$S_{vN} = -\sum_i \lambda_i \ln \lambda_i. \tag{1.5}$$

There are some properties of von Neumann entropy that are useful to note:

- A pure, separable state would yield an entropy of $S_{vN} = 0$.
- A maximally entangled state would have an entropy of $S_{vN} = \ln N$, where N is the dimension of the Hilbert space in which the state lives.
- S_{vN} is invariant under a unitary time evolution.
- If we are considering a bipartite state $|\psi\rangle$, then to apply the formula in (1.4), we must use the reduced density matrix $\rho_A = \mathrm{tr}_B |\psi\rangle\langle\psi|$. This is done similarly for tripartite states and so on.

It is with entanglement entropy where we can make a more accurate statement of the information paradox. If one computes the von Neumann entropy of the entanglement of Hawking radiation, we find that this entropy increases as the number of emitted quanta. But after a black hole completely evaporates, all that is left is the radiation which is still entangled and so is in a mixed state. But the black hole could have formed from a pure state. It is not possible to evolve from a pure state to a mixed one under unitary evolution, hence the paradox.

We should introduce the distinction between what is called 'fine-grained' entropy and 'coarse-grained' entropy in the context of black holes. Fine-grained entropy is simply the von Neumann entropy S_{vN} of the Hawking radiation. On the other hand, coarse-grained entropy (which we shall denote as S_{coarse}) is can be thought of as follows: given a system described by a density operator ρ and a set of observables O_i, we can then consider the set of density operators $\tilde{\rho}$ that give the same result for our set of observables as the first system (i.e. $\mathrm{tr}(\tilde{\rho} O_i) = \mathrm{tr}(\rho O_i)$). For any given density operator within $\tilde{\rho}$, we can calculate its von Neumann entropy $S_{vN}(\tilde{\rho})$. The coarse-grained entropy is therefore the maximum possible value of $S_{vN}(\tilde{\rho})$. [5, p. 16-17]

Again, there are some properties of coarse-grained entropy that are useful to note:

- Coarse-grained entropy obeys the second law of thermodynamics, i.e. it increases over time.
- From the definition of coarse-grained entropy, we must have $S_{vN} \leq S_{\text{coarse}}$.

The coarse-grained entropy of a black hole is given by the generalised entropy in (1.3) [5, p. 17]. We will refine this formula in chapter 3 with insights, such as those from AdS/CFT.

1.4 The Page curve

A black hole is usually formed by the gravitational collapse of matter and begins life as a pure state. So the entropy of radiation is obviously zero when black hole is first formed. As it begins to emit Hawking radiation, the emitted pairs of particles are entangled with each other as aforementioned. If we consider only the outgoing particle, we find that it is in a mixed state and so the entropy of radiation is no longer zero. We show in Chapter 2 that the entropy increases as more and more particle pairs are emitted.

But while the black hole is evaporating, the area of its event horizon is shrinking so this means that its thermodynamic entropy (given by the Bekenstein-Hawking entropy) is decreasing since it is proportional to the area of the black hole. We then run into a problem since it seems that the von Neumann entropy will become larger than the thermodynamic entropy at some point. This cannot occur since the number of degrees of freedom of the black hole is related to the thermodynamic entropy, so the entropy of radiation cannot be more than this. This means that the entropy of radiation must begin decreasing at this point, and continue to decrease to zero when the black hole completely evaporates. To summarise, we expect the entropy of Hawking radiation to follow the curve shown in Figure 1.1, called the Page curve.

In this review, we aim to discuss recent developments to methods in reproducing the Page curve. In chapter 2, we outline a derivation of the paradox which we will call the 'nice slice'

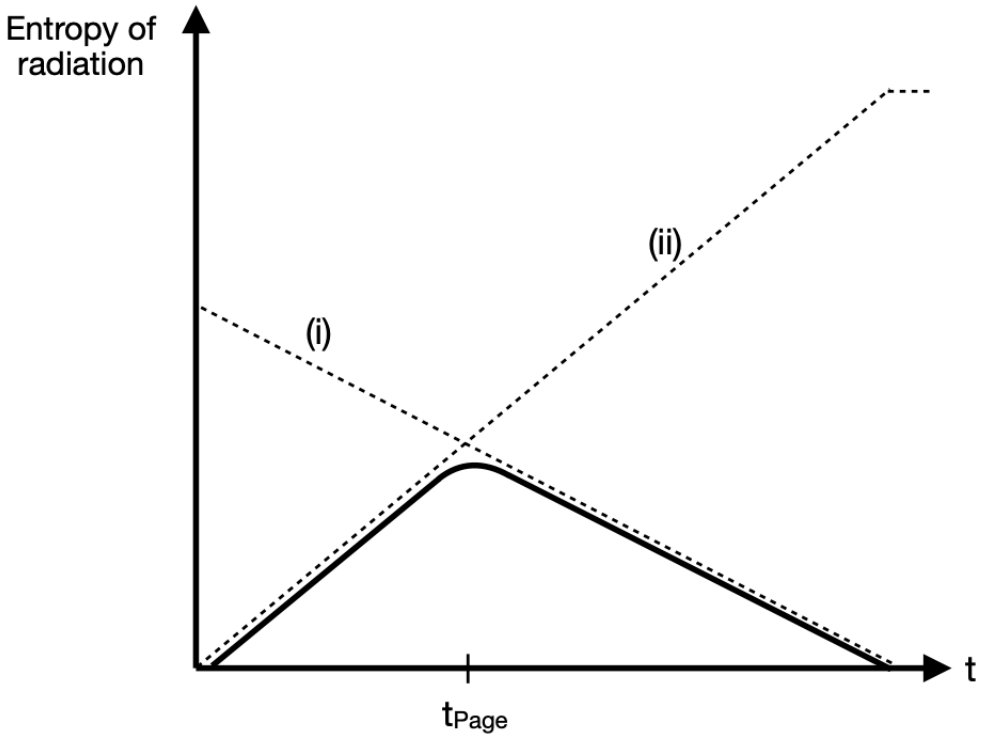

Figure 1.1: The dotted line labelled (i) represents the Bekenstein-Hawking entropy of the black hole over time, whereas the dotted line labelled (ii) represents Hawking's calculation that radiation entropy increases monotonically until evaporation. The solid line is the Page curve, and the Page time t_{Page} is the time when entropy of the Hawking radiation is equal to the Bekenstein-Hawking entropy. (Adapted from [5])

argument. The approach involves the construction of slices which satisfy certain criteria known as 'niceness conditions'. It is shown that the slices must evolve in time, i.e. are time dependent. This then gives rise to particle creation, where pairs of particle are created from the vacuum. We also discuss the effect of small corrections to the leading order of the calculation.

We discuss how the gravitational theories such as the AdS/CFT correspondence can shed some light on the paradox in chapter 3. We first provide a short introduction to the correspondence, examining the properties of both anti-de Sitter space and conformal field theories. One significant result is that the evaporation of a black hole within the framework of AdS/CFT is strictly unitary, so this suggests that unitarity must be preserved and so information is not lost in black holes. We also introduce formulae and procedures to calculate generalised entropy, which required introducing the concept of quantum extremal surfaces.

In chapter 4, we reintroduce the Page curve and apply the methods and formulae in Chapter 3 to black hole evaporation. We see how these methods lead to us recovering the Page curve. We go further with the concept of islands, and end with a brief mention of entanglement wedges and replica wormholes.

Chapter 2

The information paradox

In this chapter, we will delve into the nature of the information paradox using the slice argument, of which we will mostly follow the treatment in [7]. We will also discuss the effect of small corrections and how this affects the paradox.

2.1 The nice slice argument

Our argument involves considering spacelike slices on a Schwarzschild background around the horizon and their evolution over time. We want to work in a regime where any effects due to quantum gravity is small. To this end, we shall assume a set of 'niceness conditions', which are as follows [7, p. 2]:

- N1: The intrinsic curvature of the slice must not be larger than the Planck scale at any point of the slice.
- N2: The slice lives in a four-dimensional spacetime. The extrinsic curvature must also not be larger than the Planck scale anywhere.
- N3: The curvature of the spacetime near the slice must also be less than the Planck scale everywhere.

- N4: Matter on the slice should obey some energy condition. Quanta on the slice should not have wavelengths shorter than the Planck length, and the energy density should be less than the Planck density everywhere.

- N5: When evolving the slice to a later time, all subsequent slices must still obey the previous niceness conditions N1 to N4. Evolution must also be smooth.

A slice that obeys the niceness conditions above is henceforth referred to as a 'nice' slice.

We will now construct a nice spacelike slice on a Schwarzschild spacetime. The Schwarzschild metric is given by

$$\mathrm{d}s^2 = -\left(1 - \frac{2M}{r}\right)\mathrm{d}t^2 + \left(1 - \frac{2M}{r}\right)^{-1}\mathrm{d}r^2 + r^2\mathrm{d}\Omega_2^2, \tag{2.1}$$

with an event horizon at $r = 2M$ and a curvature singularity at $r = 0$. Recall that the event horizon is merely a coordinate singularity; an observer passing through the horizon should not observe anything out of the ordinary.

Outside the horizon at $r > 2M$, a slice segment with constant t is spacelike. On the other hand, a spacelike slice segment inside the horizon can be chosen to be a slice with constant r. In the vicinity of the horizon, these two segments are joined smoothly joined by a 'connector' segment, which can be made spacelike throughout. The entirety of the slice is illustrated in Figure 2.1.

To summarise, the construction of the nice slice is outlined as follows where, for concreteness, we shall follow the prescription in [7, p. 6]:

i. $r > 4M$: Slice segment far from horizon is given by $t = t_0$, where t_0 is a constant.

ii. $\frac{M}{2} < r < \frac{3M}{2}$: Slice segment well within horizon is given by $r = r_0$, where r_0 is a constant.

iii. $r_0 < r < 4M$: The two segments are smoothly connected by a connector segment that is spacelike everywhere.

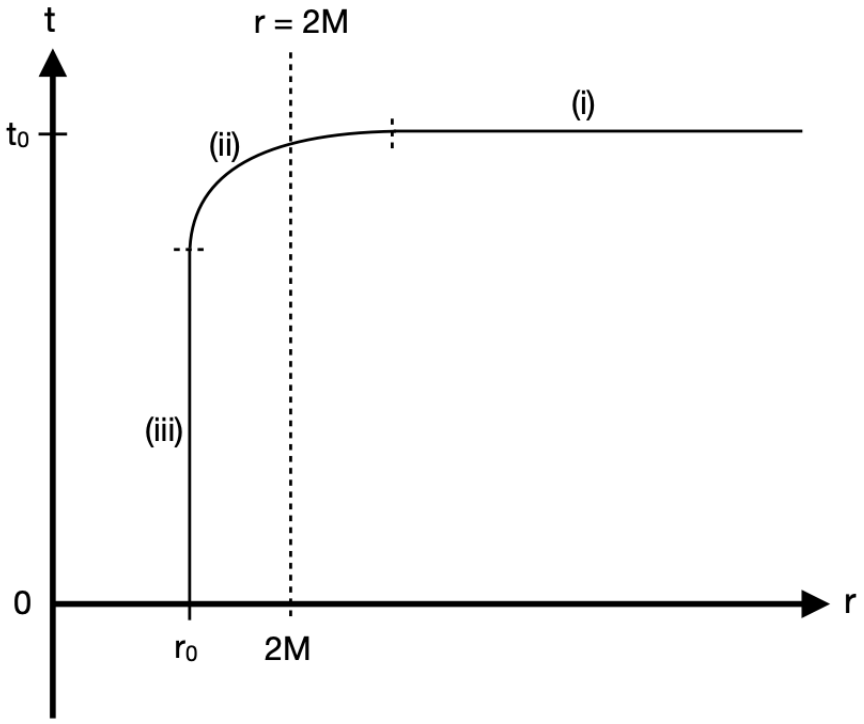

Figure 2.1: An example of a spacelike slice in a Schwarzschild background near the horizon. The segments are labelled as in the prescription above, with (ii) being the connector segment. (Adapted from [5, Fig. 2])

Now that we have constructed a nice slice, we shall now consider how it evolves in time. A slice slightly further ahead in time as the previous one is constructed as follows [7, p. 7]:

i. $r > 4M$: $t = t_1 = t_0 + \Delta$, where Δ is a constant, $\Delta > 0$ and is small.

ii. $\frac{M}{2} < r < \frac{3M}{2}$: $r = r_1 = r_0 + \delta$, where δ is a constant, $\delta < 0$, $\delta \ll M$. The radius of this segment has decreased since, within the horizon, the timelike direction is in the direction of decreasing r.

iii. $r_0 < r < 4M$: As previously, the two segments are smoothly connected by a connector spacelike segment.

This evolution of a slice over time is illustrated in Figure 2.2. We see from the figure that the slice will have to 'stretch' as it evolves over time. Specifically, it is the connector segment that has to stretch, since it has to cover the distance covered by the slice segment within the horizon whose radius has decreased. By contrast, the $t =$ const. and $r =$ const. parts of the slice remain unchanged under evolution.

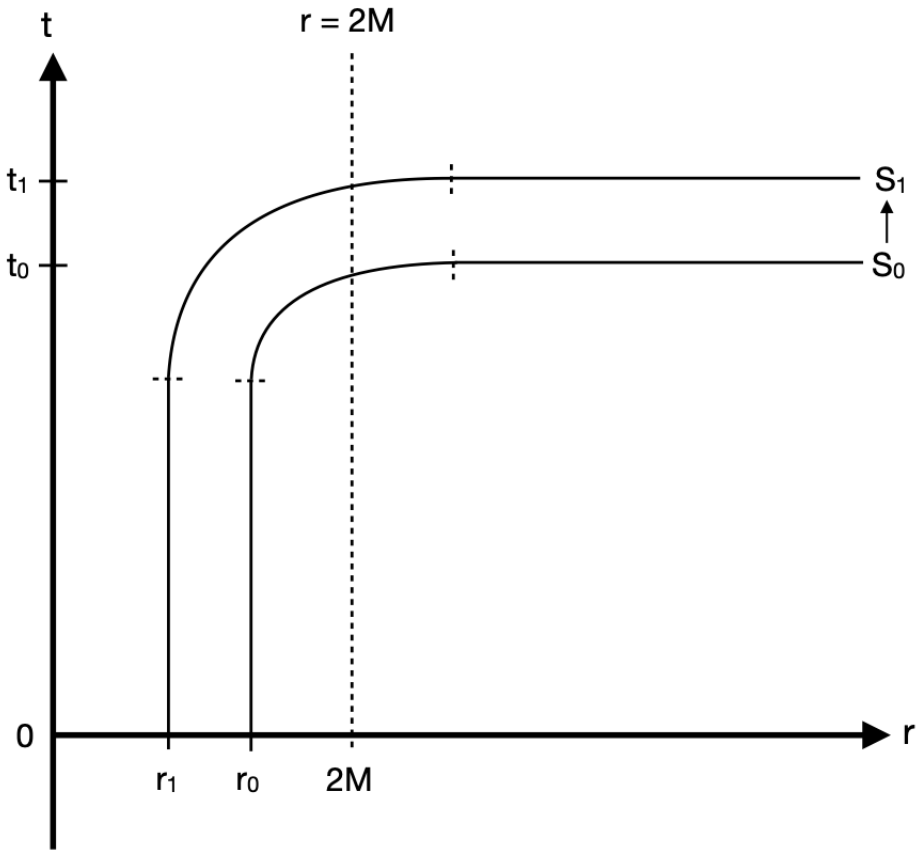

Figure 2.2: Our initial slice S_0 evolving infinitesimally to later slice S_1. Note that the connector segment has stretched, whereas the other segments are essentially unchanged. (Adapted from [5, Fig. 2])

The stretching of these spacelike slices results in pairs of particles being created from the vacuum. The connector segment lives in the vicinity of the event horizon of the black hole, so we see particle creation at the event horizon.

One might have the impression that this is a somewhat simplistic but not very useful picture. But slices (not always of the 'nice' variety) have been recently used in [8] to provide a description of the evolution of the quantum state describing a black hole. This methodology can also be extended to interacting theories as well as other metrics, including that of anti-de Sitter.

Figure 2.3 illustrates the process of particle creation. When a slice stretches, any particle pairs $\{(b_n, c_n)\}$ already on the slice is pulled apart while a new particle pair (b_{n+1}, c_{n+1}) appears in its place. The $\{c_n\}$ particles fall into the black hole, whereas the $\{b_n\}$ quanta escape into infinity as Hawking radiation. Despite this, they are still entangled with the $\{c_n\}$ particles as well as the matter state representing the black hole (represented by the black square in the Figure 2.3).

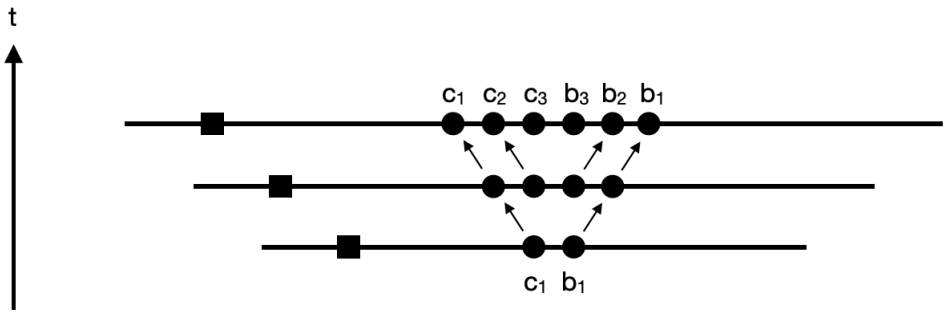

Figure 2.3: As a slice stretches, pairs of particles b_n, c_n are created. The black square represents the matter state that represents the black hole. (Adapted from [7, Fig. 4])

Let us examine how the particles are entangled throughout the process; we will mostly follow the treatment in [7, p. 11-12]. Initially, we only have the slice and the matter state, so we have $|\Psi\rangle = |\psi\rangle_M$ where we have denoted the overall state as $|\Psi\rangle$ and the matter state as $|\psi\rangle_M$. When the first particle pair (b_1, c_1) is created, the overall state is now

$$|\Psi\rangle \approx |\psi\rangle_M \otimes \left(\frac{1}{\sqrt{2}} |0\rangle_{c_1} |0\rangle_{b_1} + \frac{1}{\sqrt{2}} |1\rangle_{c_1} |1\rangle_{b_1} \right), \tag{2.2}$$

where note that b_1 and c_1 are entangled with each other. Assume that the c_1 particle falls into the black hole, whereas the b_1 particle escapes to infinity as Hawking radiationn. We can compute the von Neumann entropy of b_1 with (M, c_1), which happens to be $S_{vN} = \ln 2$. At the next timestep when the second particle pair (b_2, c_2) is created, the state is now

$$|\Psi\rangle \approx |\psi\rangle_M \otimes \left(\frac{1}{\sqrt{2}} |0\rangle_{c_1} |0\rangle_{b_1} + \frac{1}{\sqrt{2}} |1\rangle_{c_1} |1\rangle_{b_1} \right) \otimes \left(\frac{1}{\sqrt{2}} |0\rangle_{c_2} |0\rangle_{b_2} + \frac{1}{\sqrt{2}} |1\rangle_{c_2} |1\rangle_{b_2} \right). \tag{2.3}$$

As before, c_2 falls into the black hole and b_2 escapes to infinity. Now, computing the von Neumann entropy of the entanglement of $\{b_1, b_2\}$ with $\{M, c_1, c_2\}$ gives $S_{vN} = 2 \ln 2$.

We can easily generalise the state Ψ to N steps, which takes the form

$$\begin{aligned}|\Psi\rangle \approx |\psi\rangle_M \otimes &\left(\frac{1}{\sqrt{2}}|0\rangle_{c_1}|0\rangle_{b_1} + \frac{1}{\sqrt{2}}|1\rangle_{c_1}|1\rangle_{b_1}\right) \\ &\otimes \left(\frac{1}{\sqrt{2}}|0\rangle_{c_2}|0\rangle_{b_2} + \frac{1}{\sqrt{2}}|1\rangle_{c_2}|1\rangle_{b_2}\right) \\ &\vdots \\ &\otimes \left(\frac{1}{\sqrt{2}}|0\rangle_{c_N}|0\rangle_{b_N} + \frac{1}{\sqrt{2}}|1\rangle_{c_N}|1\rangle_{b_N}\right). \end{aligned} \tag{2.4}$$

Now, the von Neumann entropy of the entanglement of $\{b_1, \ldots, b_N\}$ with $\{M, c_1, \ldots, c_N\}$ gives the general result

$$S_{vN} = N \ln 2, \tag{2.5}$$

so, in general, the von Neumann entropy increases by $\ln 2$ each time a new particle pair is created [7, p. 11-12]. We now see how the information paradox arises. When the black hole completely evaporates, we are left with the quanta $\{b_1, \ldots, b_N\}$ which have an entanglement entropy of $N \ln 2 \neq 0$. As we previously mentioned briefly, a problem arises in that we arrived at a nonzero entropy from an initial state that was pure. This is not possible under unitary evolution as we stated in the previous chapter, so it seemingly

2.2 The effect of small corrections

We saw in the previous section how evolving the initial state/slice leads to a nonzero entropy. But this is a leading order calculation that does not take into account small corrections, which for instance can arise from interactions between different pairs of particles [7, p. 14]. As a result, it was conjectured that small corrections to the state Ψ would be sufficient to remove the paradox. In this section, we shall discuss two opposing arguments regarding this matter.

One argument is made in [7] which says that small corrections to the leading order calculation in the previous section will not fundamentally change our conclusion that unitarity is violated. We will closely follow that argument here. Recall that we are mainly interested in the subsystems

$\{b\}$ and $\{M, c\}$, which are entangled with each other. Let us write our state $|\Psi\rangle$ at timestep t_n as $|\psi_{M,c}, \phi_b(t_n)\rangle$. Now, at the next timestep t_{n+1}, a new particle pair is created so we can write the evolution of the state $|\Psi\rangle$ from t_n to t_{n+1} as

$$|\psi_{M,c}, \phi_b(t_n)\rangle \to |\psi_{M,c}, \phi_b(t_{n+1})\rangle = |\psi_{M,c}, \phi_b(t_n)\rangle \left(\frac{1}{\sqrt{2}} |0\rangle_{c_{n+1}} |0\rangle_{b_{n+1}} + \frac{1}{\sqrt{2}} |1\rangle_{c_{n+1}} |1\rangle_{b_{n+1}} \right), \tag{2.6}$$

where as usual the new particle pair is an entangled state. To take into account small corrections during the particle creation process, we assume that the newly created state representing the new particle pair lives in a space spanned by the orthonormal vectors given by

$$\begin{aligned} |V_1\rangle &= \frac{1}{\sqrt{2}} |0\rangle_{c_{n+1}} |0\rangle_{b_{n+1}} + \frac{1}{\sqrt{2}} |1\rangle_{c_{n+1}} |1\rangle_{b_{n+1}} \\ |V_2\rangle &= \frac{1}{\sqrt{2}} |0\rangle_{c_{n+1}} |0\rangle_{b_{n+1}} - \frac{1}{\sqrt{2}} |1\rangle_{c_{n+1}} |1\rangle_{b_{n+1}}. \end{aligned}$$

Next, we choose orthonormal bases for the two subsystems $\{M, c\}$ and $\{b\}$ as $\{|\chi_i\rangle\}$ and $\{|\xi_i\rangle\}$ respectively. This allows us to write the state at time t_n as

$$|\psi_{M,c}, \phi_b(t_n)\rangle = \sum_{m,n} C_{mn} |\chi_m\rangle |\xi_n\rangle, \tag{2.7}$$

where C_{mn} is a set of constants. We can perform a transformation to $\{\chi_i\}$ and $\{\xi_i\}$ such that we obtain

$$|\psi_{M,c}, \phi_b(t_n)\rangle = \sum_i C_i |\chi_i\rangle |\xi_i\rangle. \tag{2.8}$$

Computing the reduced density matrix $\rho_b(t_n)$ representing just the $\{b\}$ subsystem, we obtain

$$\hat{\rho}_b(t_n) = |C_i|^2 \, \hat{1}, \tag{2.9}$$

so from (1.5) we can compute the von Neumann entropy at time t_n to be

$$S_{vN}(t_n) = -\sum_i |C_i|^2 \ln |C_i|^2. \tag{2.10}$$

We now want to consider evolution by one timestep to t_{n+1} and its effect on the von Neumann

entropy in (2.10). The most general possible evolution is given by

$$|\xi_i\rangle \to |\xi_i\rangle \tag{2.11}$$

$$|\chi_i\rangle \to |\chi_{i,1}\rangle|V_1\rangle + |\chi_{i,2}\rangle|V_2\rangle. \tag{2.12}$$

The reason why $|\xi_i\rangle$ is unchanged is that we can consider the $\{b\}$ quanta to have escaped the hole and thus is no longer influenced by it. On the other hand, the $\{M, c\}$ subsystem has evolved to include the newly created pair represented by $|V_1\rangle$ and $|V_2\rangle$. Note that we must have

$$\||\chi_{i,1}\rangle\|^2 + \||\chi_{i,2}\rangle\|^2 = 1, \tag{2.13}$$

with our leading order calculation being the special case $|\chi_{i,1}\rangle = |\chi_i\rangle$ and $|\chi_{i,2}\rangle = 0$.

Using (2.11) and (2.12), we can evolve (2.8) to time t_{n+1} which gives

$$|\psi_{M,c}, \phi_b(t_{n+1})\rangle = \sum_i C_i\Big(|\chi_{i,1}\rangle|V_1\rangle + |\chi_{i,2}\rangle|V_2\rangle\Big)|\xi_i\rangle \tag{2.14}$$

$$= |V_1\rangle\left(\sum_i C_i|\chi_{i,1}\rangle|\xi_i\rangle\right) + |V_2\rangle\left(\sum_i C_i|\chi_{i,2}\rangle|\xi_i\rangle\right) \tag{2.15}$$

$$= |V_1\rangle|\Lambda_1\rangle + |V_2\rangle|\Lambda_2\rangle, \tag{2.16}$$

where we have defined

$$|\Lambda_1\rangle = \sum_i C_i|\chi_{i,1}\rangle|\xi_i\rangle, \quad |\Lambda_2\rangle = \sum_i C_i|\chi_{i,2}\rangle|\xi_i\rangle. \tag{2.17}$$

Note that we have

$$\||\Lambda_1\rangle\|^2 + \||\Lambda_2\rangle\|^2 = 1 \tag{2.18}$$

since $|V_1\rangle$ and $|V_2\rangle$ are both orthonormal and $|\psi_{M,c}, \phi_b(t_{n+1})\rangle$ is normalised. We can finally define corrections to the leading order calculation to be small if

$$\||\Lambda_2\rangle\| < \epsilon, \quad \epsilon \ll 1. \tag{2.19}$$

Let us now consider the whole system at time t_{n+1}. We have three subsystems: the emitted quanta $\{b\} \equiv \{b_1, \ldots, b_n\}$, the black hole interior $\{M, c\} \equiv \{M, c_1, \ldots, c_n\}$, and the newly created pair $p \equiv (b_{n+1}, c_{n+1})$. Now, if we are considering the entropy of some subsystem A with the other two subsystems B and C, we will denote this as $S_{vN}(A) \equiv -\mathrm{tr}(\rho_A \ln \rho_A)$. By this notation, (2.10) can be written as

$$S_{vN}(\{b\}) = -\sum_i |C_i|^2 \ln |C_i|^2. \tag{2.20}$$

In [7, p. 18-19], the three following inequalities were proven:

$$S_{vN}(p) < \epsilon \tag{2.21}$$

$$S_{vN}(\{b\} + p) \geq S_{vN}(\{b\}) - \epsilon \tag{2.22}$$

$$S_{vN}(c_{n+1}) > \ln 2 - \epsilon, \tag{2.23}$$

of which we will not reproduce the proof here for the sake of brevity. Note that (2.21) shows how the new pair $p \equiv (b_{n+1}, c_{n+1})$ is very weakly entangled with the rest of the system.

We now apply the strong subadditivity theorem for a system with three subsystems A, B, and C which is given by

$$S_{vN}(A + B) + S_{vN}(B + C) \geq S_{vN}(A) + S_{vN}(C). \tag{2.24}$$

Setting $A = \{b\}, B = b_{n+1}, C = c_{n+1}$ whilst noting that $p = B + C$, we have

$$\begin{aligned} &S_{vN}(\{b\} + b_{n+1}) + S_{vN}(p) \geq S_{vN}(\{b\}) + S_{vN}(c_{n+1}) \\ &\quad \implies S_{vN}(\{b\} + b_{n+1}) \geq S_{vN}(\{b\}) + S_{vN}(c_{n+1}) - S_{vN}(p). \end{aligned}$$

Using the inequalities (2.21) and (2.23), we finally arrive at the inequality for governing the entropy for all of the emitted quanta $\{b_1, \ldots, b_{n+1}\}$ with the rest of the black hole interior,

which is

$$S_{vN}(\{b\} + b_{n+1}) \geq S_{vN}(\{b\}) + \ln 2 - 2\epsilon. \tag{2.25}$$

Recalling that $\epsilon \ll 1$ if leading order corrections are small, we conclude that the von Neumann entropy of emitted quanta must increase by at least $\ln 2 - 2\epsilon$ each time a new particle pair is created, and so our original conclusion is unaffected when taking into account small corrections.

Chapter 3

Entanglement entropy in gravitational theories

In this chapter we shall review notions of entropy in the framework of the conjecture known as AdS/CFT (also called gauge-gravity duality). AdS/CFT is a conjecture first proposed by Juan Maldacena in 1998 [9]. AdS refers to anti-de Sitter space, whereas CFT stands for conformal field theory. AdS/CFT remains a conjecture for now, but there are indications that it is correct [10].

It is the most successful realisation of the holographic principle, which was first proposed by Gerard t'Hooft in the context of quantum gravity [11] and given a precise formulation by Leonard Susskind [12]. The principle essentially states that a feature of quantum gravity is that a volume of space can be described as being encoded on its boundary.

We will first review the key features of AdS/CFT, first by examining the features of anti-de Sitter space and conformal field theories in turn, which will then allow us to make a precise statement of what AdS/CFT is. We then explain what inferences can be made from AdS/CFT to shine some light on the information paradox. The main result is that one can create a black hole state and evolve it forwards in time, where it is found that this evolution is unitary [13, p. 87]. This means that if AdS/CFT is true, then black hole evaporation is indeed unitary. After reviewing AdS/CFT, we will introduce the Ryu-Takayanagi formula which provides an

expression for fine-grained entropy within AdS/CFT.

3.1 Anti-de Sitter space

Anti-de Sitter (AdS) space is a maximally symmetric space with a constant negative Ricci scalar curvature and a negative cosmological constant that is a solution of Einstein's equations[1]. One form of the metric is given by

$$\mathrm{d}s^2 = -f\mathrm{d}t^2 + \frac{1}{f}\mathrm{d}r^2 + r^2\mathrm{d}\Omega_{d-1}^2, \tag{3.1}$$

where $f = 1 + \left(\frac{r}{r_{AdS}}\right)^2$, $t \in (\infty, \infty), r \in [0, \infty)$. Here r_{AdS} is a length which relates to the vacuum energy ρ_0 by

$$\frac{1}{r_{AdS}^2} = -\frac{16\pi G\rho_0}{d(d-1)}, \tag{3.2}$$

but we can simplify things by setting $r_{AdS} = 1$, which we will do from now on [13, p. 69].

Let us examine some properties of AdS spacetime. It asymptotically approaches Minkowski space for $r \ll 1$, but not as $r \to \infty$. It is useful to note that, analogously to flat space, there exists a notion of asymptotically AdS spacetime. Put simply, an asymptotically AdS spacetime approaches AdS as r tends to infinity, and its boundary is timelike [13, p. 69-70].

To examine its behaviour of AdS as r tends to infinity, we can perform the substitution $r = \tan\rho$, which transforms (3.1) into

$$\mathrm{d}s^2 = \frac{1}{\cos^2\rho}(-\mathrm{d}t^2 + \mathrm{d}\rho^2 + \sin^2\rho\,\mathrm{d}\Omega_{d-1}^2), \tag{3.3}$$

where $\rho \in [0, \frac{\pi}{2})$. We can compactify by including $\rho = \frac{\pi}{2}$ which represents the boundary, but we see that (3.3) shows that AdS space is topologically equivalent to $\mathbb{R} \times \mathbb{S}^{d-1}$ (a d-dimensional 'cylinder'). We also see from the metric that massless particles moving outwards in ρ would (on this cylinder) move diagonally towards the boundary, at which point it will return to where it

[1] Its counterpart is de Sitter space, which has a positive cosmological constant.

came from. On the other hand, massive particles moving outwards would move away for some distance without reaching the boundary and then turn around to return to its origin [13, p. 69]. This is all illustrated in Figure 3.1.

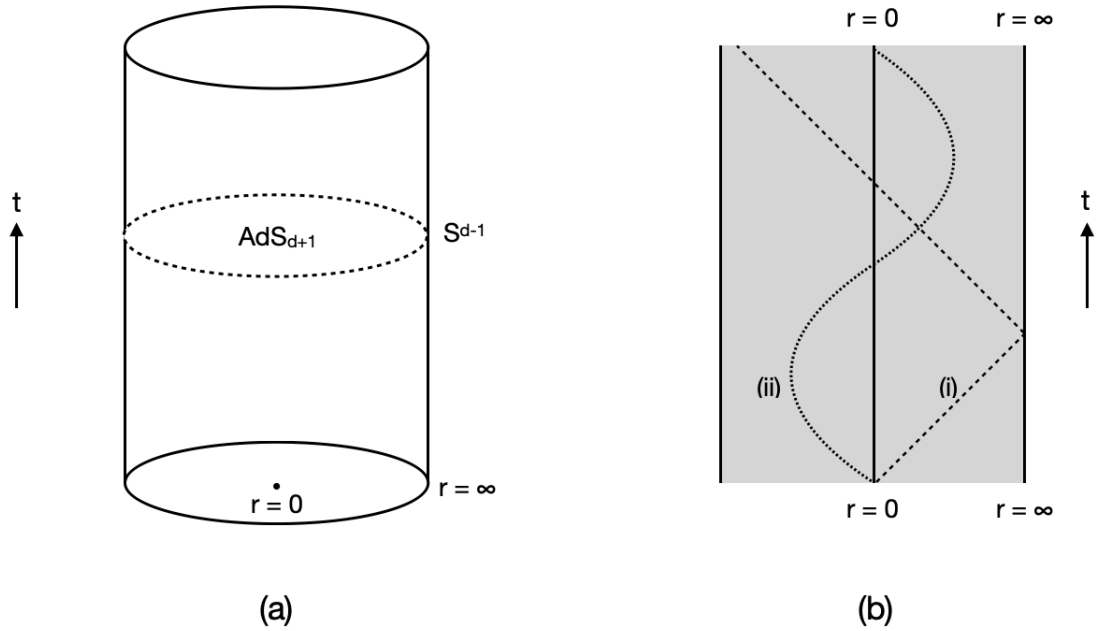

Figure 3.1: (a) The Penrose diagram for anti-de Sitter space, with a $(d-1)$-sphere represented as a circle (Adapted from [10, Fig. 1]). (b) A slice of the Penrose diagram showing a: (i) massless geodesic (ii) massive geodesic.

3.2 Conformal field theory

Recall that the Poincaré group is the group that keeps the Minkowski metric $\eta_{\mu\nu}$ invariant. This means symmetry under translations and Lorentz transformations (rotations + boosts), whose action on a spacetime coordinate x^μ is given respectively by

$$x^\mu \to x'^\mu = x^\mu - a^\mu \tag{3.4}$$

$$x^\mu \to x'^\mu = \Lambda^\mu{}_\nu x^\nu, \tag{3.5}$$

where $\Lambda^\mu{}_\nu \in SO(1, d-1)$ and a^μ is some constant translation [13, p. 70-71]. The Poincaré group is generated by the translation and Lorentz generators P_μ and $M_{\mu\nu}$ respectively, which

form the Poincaré algebra given by

$$[M_{\mu\nu}, P_\alpha] = -i(\eta_{\mu\alpha}P_\nu - \eta_{\nu\alpha}P_\mu) \tag{3.6}$$

$$[M_{\mu\nu}, M_{\alpha\beta}] = -i(\eta_{\mu\alpha}M_{\nu\beta} - \eta_{\mu\beta}M_{\nu\alpha} - \eta_{\nu\alpha}M_{\mu\beta} + \eta_{\nu\beta}M_{\mu\alpha}). \tag{3.7}$$

We can consider another type of symmetry which is scale symmetry. A theory that has scale symmetry is invariant under a scaling transformation (also known as a dilation or dilatation), whereby a spacetime coordinate x^μ transforms as

$$x^\mu \to \lambda x^\mu, \tag{3.8}$$

where $\lambda \neq 1$ is some real number. Dilations are generated by the dilation operator D which acts on a function $f(x)$ as

$$Df(x) = ix^\mu \partial_\mu f, \tag{3.9}$$

and commutes with $M_{\mu\nu}$ but also obeys

$$[P_\mu, D] = iP_\mu. \tag{3.10}$$

A field can scale in different ways but in general it transforms as

$$\phi(x) \to \phi'(x) = \lambda^\Delta \phi(\lambda x), \tag{3.11}$$

where Δ is known as the scaling dimension of the field [13, p. 71].

The final type of symmetry we need to consider is symmetry under a special conformal transformation, which is given by

$$x^\mu \to \frac{x^\mu + a^\mu x^2}{1 + 2x^\mu a_\mu + a^2 x^2}, \tag{3.12}$$

where a^μ is some constant spacetime vector. Essentially, it is the composition three transformations: an inversion $x^\mu \to \frac{x^\mu}{x^2}$, a translation $x^\mu \to x^\mu + a^\mu$, and a second inversion in that order. Special conformal transformations are generated by a generator K_μ, which acts on a

function $f(x)$ as [13, p. 70-71]

$$K_\mu f(x) = i(x^2\partial_\mu - 2x_\mu x^\nu \partial_\nu)f. \tag{3.13}$$

The conformal group is therefore the group which is symmetric under all three transformations: Poincaré, dilation and special conformal. It is the set of transformations of Minkowski space that preserves angles (but not always lengths) and is isomorphic to $SO(d,2)$ [13, p. 71]. This group is then generated by the generators $P_\mu, M_{\mu\nu}, D, K_\mu$ which form an algebra given by

$$[D, K_\mu] = iK_\mu \tag{3.14}$$

$$[P_\mu, K_\mu] = 2i(M_{\mu\nu} - \eta_{\mu\nu}D) \tag{3.15}$$

$$[M_{\mu\nu}, K_\alpha] = -i(\eta_{\mu\alpha}K_\nu - \eta_{\nu\alpha}K_\mu) \tag{3.16}$$

in addition to the ones in (3.4), (3.5) and (3.10). A conformal field theory is therefore some field theory that is invariant under the conformal group. One simple example of a conformal field theory is the free massless scalar field [13, p. 71].

Conformal field theory is a massive topic and is a whole field of study in itself, but we shall examine two important properties here. One property of CFTs is that we can always find a set of operators called primary operators, which we shall denote as $\mathcal{O}(x)$. These operators commute with the generators of special conformal transformation when $x = 0$ and also transform under dilations as

$$\mathcal{O}(x) \to \mathcal{O}'(x') = \lambda^{-\Delta}\mathcal{O}(x), \tag{3.17}$$

where Δ is the conformal dimension of the primary operator. A CFT is unitary if Δ is real and positive, whereas $\mathcal{O}(x)$ is a scalar operator if $\Delta \geq \frac{d-2}{2}$ [13, p. 71]. The correlation functions of primary operators are very simple. For example, the time-ordered two point correlation function for a primary operator takes the form

$$\langle\Omega|\hat{T}\mathcal{O}(x,t)\mathcal{O}(0,0)|\Omega\rangle = \frac{1}{(|x|^2 - t^2 + i\epsilon)^\Delta}. \tag{3.18}$$

Another property of CFTs is something called the state-operator correspondence. Given some Hamiltonian, we have a set of energy eigenstates. In any CFT, we have a natural bijection between these energy eigenstates and operators that act locally, i.e. in the neighbourhood of the origin. This bijection is what is known as the state-operator correspondence. It arises from studying CFTs on the cylindrical space $\mathbb{R} \times \mathbb{S}^{d-1}$ with metric

$$\mathrm{d}s^2 = -\mathrm{d}t^2 + \mathrm{d}\Omega_{d-1}^2. \tag{3.19}$$

We then consider the Euclidean metric $\mathbb{R}^d$ written as

$$\mathrm{d}s^2 = \mathrm{d}\rho^2 + \rho^2 \mathrm{d}\Omega_{d-1}^2. \tag{3.20}$$

Taking $\rho = e^\tau$, (3.20) then becomes

$$\mathrm{d}s^2 = e^{2\tau}(\mathrm{d}\tau^2 + \mathrm{d}\Omega_{d-1}^2), \tag{3.21}$$

where we see that it is equivalent to (3.19) after a Weyl transformation as well as a Wick rotation $\tau = it$ [13, p. 71-72].

3.3 AdS/CFT and the information paradox

Now that we have introduced both sides of AdS/CFT correspondence, we can provide a precise statement of it [13, p. 73]:

- Any relativistic conformal field theory on $\mathbb{R} \times \mathbb{S}^{d-1}$ with metric (3.19) can be interpreted as a theory of quantum gravity in an asymptotically $AdS_{d+1} \times M$ spacetime. Here M is some compact manifold that may or may not be trivial.

Put simply, it posits that there exists a duality between certains CFTs and theories of quantum gravity in AdS spaces. Often we refer to some AdS description as the 'bulk' theory whereas the

CFT is called the 'boundary' theory. Now, the statement above reads like a definition but, as mentioned at the start of this chapter, it remains a conjecture although there exists evidence pointing towards its validity.

So how does this mapping work? The simple answer is that bulk fields are mapped to a CFT via a 'dictionary'. For example, one important 'entry' in this dictionary is the extrapolate dictionary which describes how a bulk field can be extrapolated to the boundary where we obtain some quantity that corresponds to a primary operator in the CFT [13, p. 73-74].

Turning our attention back to black holes, we note that there exists a black hole solution in AdS which has metric

$$\mathrm{d}s^2 = -f(r)\mathrm{d}t^2 + \frac{1}{f(r)}\mathrm{d}r^2 + r^2\mathrm{d}\Omega_{d-1}^2, \tag{3.22}$$

where

$$f(r) = r^2 + 1 - \frac{\alpha}{r^{d-2}} \tag{3.23}$$

and we have set $r_{AdS} = 1$ as usual. Here α is a constant that is related to mass M by

$$\alpha = \frac{16\pi GM}{(d-1)\Omega_{d-1}}. \tag{3.24}$$

Now, the main inference we can make from what we know in AdS/CFT is that Hawking radiation (by virtue of being massless) can reach the boundary and be reflected back to where it originated. This means that a black hole in AdS spacetime eventually reabsorbs the radiation it emitted. Of course, a black hole may evaporate completely long before any radiations returns to it. This leads us to the notion of 'big' and 'small' black holes in AdS, where 'big' AdS black holes are those which are large enough such that radiation is reflected back to the black hole as fast as it emits them. These black holes therefore never evaporate and so are also called 'eternal' black holes. By contrast, 'small' black holes are those that eventually evaporate as usual.

We can derive the regimes at which black holes are big or small. A given black hole with energy E will have some fraction x of its energy in the black hole, with the rest being in

emitted radiation. The total entropy of the system is given by

$$S \approx (El_p)^2 x^2 + (Er_{AdS})^{\frac{3}{4}}(1-x)^{\frac{3}{4}}, \tag{3.25}$$

where the first term on the right hand side represents the entropy of the black hole and the second term represents the entropy of radiation [13, p. 78-79].

We want to find x when S is maximised. At low E, the second term dominates so it is maximised at $x = 0$, which means there is no black hole. On the other hand, at large enough E, the first term dominates so S is maximised when x is close to but not exactly 1. This is when almost all the energy is contained within a black hole which is eternal. So we showed that a black hole becomes eternal at large enough E. This threshold can be found by finding when the two terms in (3.25) are comparable. This is when the energy satisfies [13, p. 79]

$$Er_{AdS} = \left(\frac{r_{AdS}}{l_p}\right)^2 \left(\frac{r_{AdS}}{l_p}\right)^{-\frac{2}{5}}. \tag{3.26}$$

We now have the tools needed to consider the information paradox within the context of AdS/CFT. Using creation operators within a CFT, we can form a shell of matter that we know will collapse to create a black hole. We need to specify that the black hole is small enough to evaporate, which means we have

$$Er_{AdS} \ll \left(\frac{r_{AdS}}{l_p}\right)^{-\frac{d^2-1}{2d-1}}, \tag{3.27}$$

but it also has to be large enough to be semiclassical which means

$$Er_{AdS} \gg \frac{r_{AdS}}{l_p}. \tag{3.28}$$

Once we have formed our black hole, we can evolve it forward in time within the CFT. This evolution is always unitary, so we can conclude that the answer to the paradox is that information is preserved. It should be noted this does not yet say anything about the mechanism

in which unitarity is preserved [13, p. 87].

3.4 Fine-grained entropy in AdS/CFT

We can now switch our attention to entropy. Recall in Chapter 1 that we introduced the notions of fine and coarse-grained entropy. In 2006, Shinsei Ryu and Tadashi Takayanagi proposed a way to compute the von Neumann (fine-grained) entropy within the case $\mathrm{AdS}_3/\mathrm{CFT}_2$ [14]. The idea is that given our CFT lives on the space $\mathbb{R} \times \mathbb{S}^{d-1}$, we pick out some Cauchy slice with topology $\mathbb{S}^{d-1}$ and examine some state from the CFT on it. We can consider dividing the slice into two regions A and B and computing the entanglement entropy S_A for region A. This would as usual be given by [14, p. 1]

$$S_A = -\mathrm{tr}(\rho_A \ln \rho_A), \tag{3.29}$$

where

$$\rho_A = \mathrm{tr}_B(|\Psi\rangle\langle\Psi|). \tag{3.30}$$

But Ryu and Takayanagi proposed that S_A can be computed with the formula

$$S_A = \frac{\text{Area of } \gamma_A}{4G_N^{(d+2)}}, \tag{3.31}$$

where γ_A is a d-dimensional static minimal surface whose boundary is ∂A and $4G_N^{(d+2)}$ is the $(d+2)$-dimensional Newton's constant. This formula has been found to obey properties that entropy also should, such as strong subadditivity and monogamy of mutual information [15].

We can extend this to a 'generalised' entropy which includes the entropy of external fields. As before, this will be calculated on some surface such that the surface minimises the entropy. This minimal entropy is therefore the value for the fine-grained entropy. We can encapsulate

this with the 'formula' [5, p. 10]

$$S \sim \min \left[\frac{\text{Area}}{4G_N} + S_{\text{outside}} \right]. \tag{3.32}$$

But what we really want is to extremise the surface not only in space, but in time. More accurately, we want to minimise it in the spatial direction but maximise it in the temporal direction. Such a surface is then an 'extremal surface'. This is done by choosing some Cauchy slice, finding the minimal surface on it, and then finding the Cauchy slice with the maximum value for its minimal surface [5, p. 10]. We can write this as

$$S(X) = \min_X \left\{ \text{ext}_X \left[\frac{\text{Area}(X)}{4G_N} + S_{\text{sc}}(\Sigma_X) \right] \right\}, \tag{3.33}$$

where X is a surface of codimension 2 (it has dimension two fewer than that of the spacetime it lives in), Σ_X is the region bounded by X and $S_{\text{sc}}(\Sigma_X)$ is the von Neumann entropy of quantum fields living on Σ_X. We then call the surface that extremises (3.33) a 'quantum extremal surface' since it takes into account the external quantum fields [5, p. 10-11]. This procedure is illustrated in 3.2. In the next chapter, we will see how this generalised entropy reproduces the Page curve.

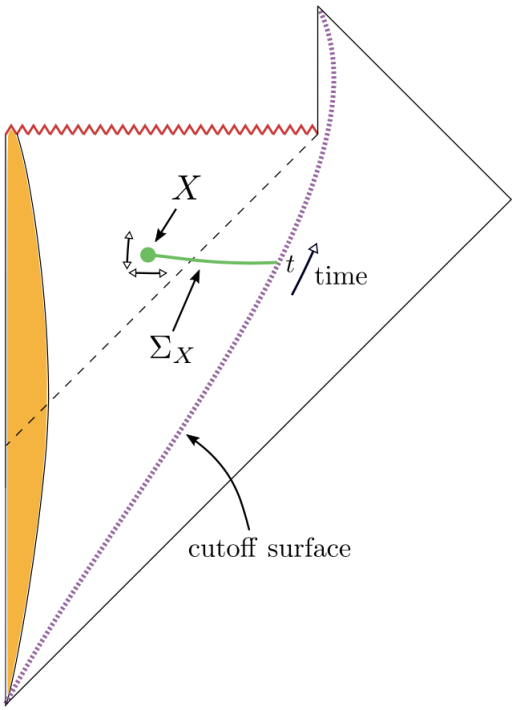

Figure 3.2: How to find the quantum extremal surface for a black hole. We start on some imaginary cutoff surface where surface X is varied until the entropy is extremised. Note that a point on the diagram represents a 2-sphere. (Image credit: [5, Fig. 8])

Chapter 4

The Page curve

In this section, we will further explore the Page curve, which we introduced in Chapter 1. We first reiterate qualitatively how it arises, and then apply the methods in the previous chapter to show how the Page curve can be reproduced.

4.1 Deriving the Page curve

Recall in Chapter 1 that we reasoned that the entropy of Hawking radiation should follow the Page curve as shown in Figure 4.1. Essentially, we said that the entropy of radiation is zero at the start. and increases as it begins to emit Hawking radiation. We then noted that the thermodynamic entropy decreases as the black hole evaporates since its area is shrinking. This meant that the entropy of radiation decreases after the Page time since the entropy of radiation cannot be greater than the thermodynamic entropy of the black hole. This was because the thermodynamic entropy is related to the number of degrees of freedom of the black hole.

Overall, our motivation for the shape of the Page curve is that black hole evaporation should be unitary. This idea can be restated in more specific terms in a principle known as the 'central dogma'[1]. It can be stated as follows [5, p. 5]:

[1]This name is derived from biology where it pertains to the flow of genetic information [5, p. 7]

Figure 4.1: An approximate profile for how the Page curve should look like. For black hole evaporation to be truly unitary, the entropy must The entropy of radiation is maximised at t_{Page}.

- As seen from the outside, a black hole can be described in terms of a quantum system with Area/$(4G_N)$ degrees of freedom that evolves unitarily under time evolution.

Note that this statement makes no assumptions about the black hole interior. By 'degrees of freedom', we mean more specifically that it is related to the logarithm of the dimension of the Hilbert space. Since the number of degrees of freedom is finite, we therefore have that the Hilbert space dimension is also finite. We should also note that, although quantum effects become significant when the black hole is about to evaporate completely (when its radius is comparable to a Planck length), the argument still remains since we first conflicted with the central dogma at the Page time when the black hole isn't small [5, p. 5-9]

4.2 Reproducing the Page curve

We now turn our attention to efforts in finding a mechanism that reproduces the Page curve. Recall we introduced the formula for finding the fine-grained entropy in the previous chapter given by

$$S(X) = \min \left\{ \text{ext} \left[\frac{\text{Area}(X)}{4G_N} + S_{\text{sc}}(\Sigma_X) \right] \right\}, \tag{4.1}$$

where we calculate this on a quantum extremal surface X. We shall now apply this procedure to an evaporating black hole and see how the resultant entropy varies throughout the lifetime of the black hole.

When the black hole first forms, it happens to be that the extremal surface is vanishing, so the first term in (4.1) is zero. This is illustrated in Figure 4.2. But the second term is also zero if the collapsing matter that formed the black hole is a pure state. Therefore $S = 0$ at the start. By contrast, the thermodynamic entropy is nonzero shortly after the black hole forms since the area is nonzero. When the black hole begins to emit Hawking radiation, the von Neumann entropy begins increasing whereas the thermodynamic entropy starts decreasing [5, p. 11]. This is all illustrated in Figure 4.3

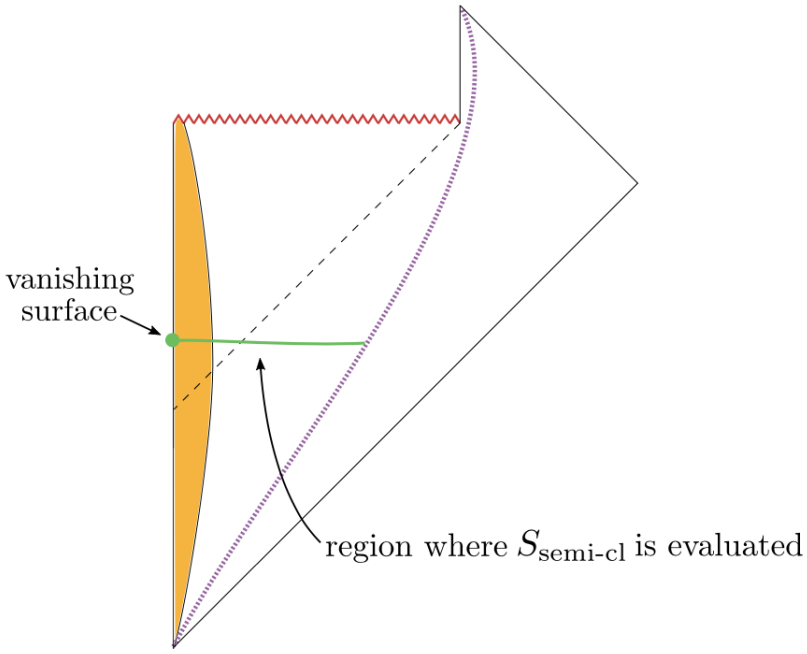

Figure 4.2: At early times, the minimal surface of the black hole is zero, also known as the vanishing surface. (Image credit: [5, Fig. 9])

But this is complicated by the fact that a non-vanishing extremal surface appears shortly after evaporation begins. Where exactly the quantum extremal surface appears depends on the amount of radiation already emitted and so is time-dependent. In fact, it lies close to the black hole event horizon [5, p. 11].

We determine the location of the quantum extremal surface by moving back in time from a

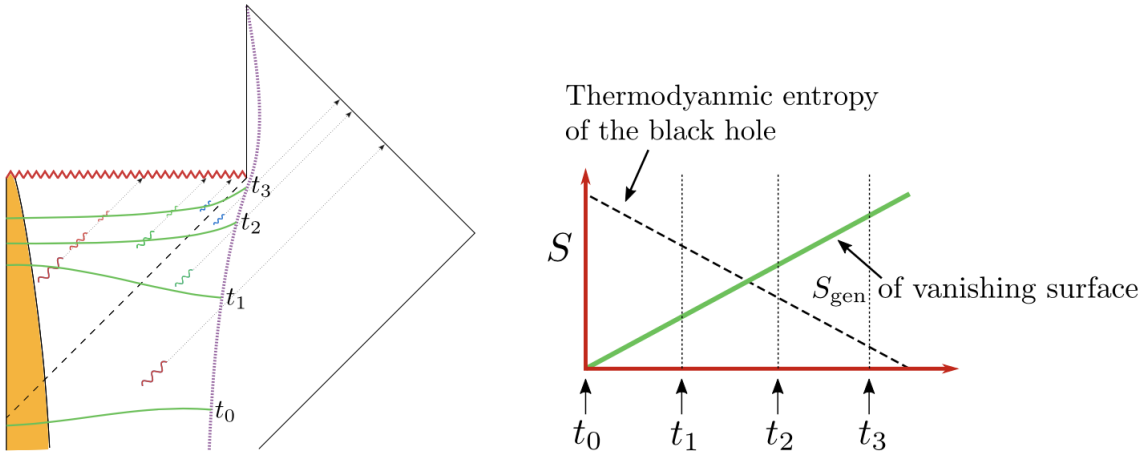

Figure 4.3: Left: Vanishing surfaces at different times. Right: In the case of vanishing surfaces, $S(X)$ is zero at the start, but increases as Hawking radiation is emitted. By contrast, thermodynamic entropy decreases over time. (Image credit: [5, Fig. 10])

given point on the cutoff surface by an amount $r_S \ln S_{BH}$ and releasing an ingoing light ray. Where the ray meets the event horizon is where the quantum extremal surface is close to. This means that $S(X)$ is approximately equal to the area term, which means that it decreases over time just like for thermodynamic entropy. The quantity $r_S \ln S_{BH}$ is known as the 'scrambling' time [5, p. 11-12]. This is all shown in Figure 4.4.

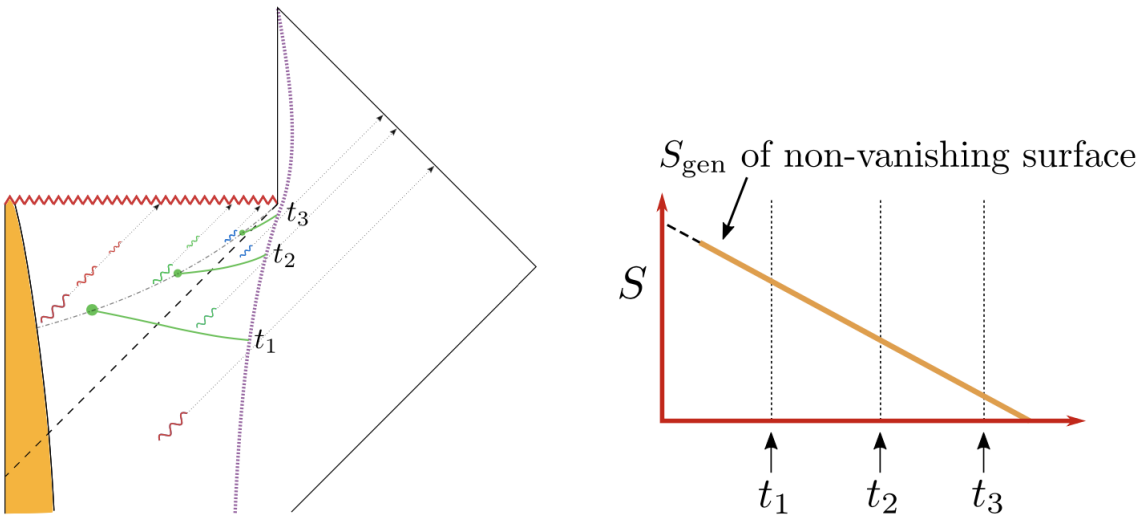

Figure 4.4: Left: non-vanishing surfaces at different times on the cutoff surface, the first of which is situated near the horizon but inside the black hole. Right: In the case of non-vanishing surfaces, S(X) decreases over time. (Image credit: [5, Fig. 11])

The last thing to do is to minimise over all possible extremal surfaces, so real generalised entropy

is found by taking the minimum of the entropy for either the vanishing or non-vanishing case at all times. This leads to the Page curve shown in the right figure in Figure 4.5. The left figure in Figure 4.5 shows how we initially start with a vanishing surface and then eventually a non-vanishing surface is created. We transition from using a vanishing surface to a non-vanishing one when the entropy calculated from a non-vanishing surface is smaller than that of its vanishing counterpart, which occurs at the Page time [5, p. 13].

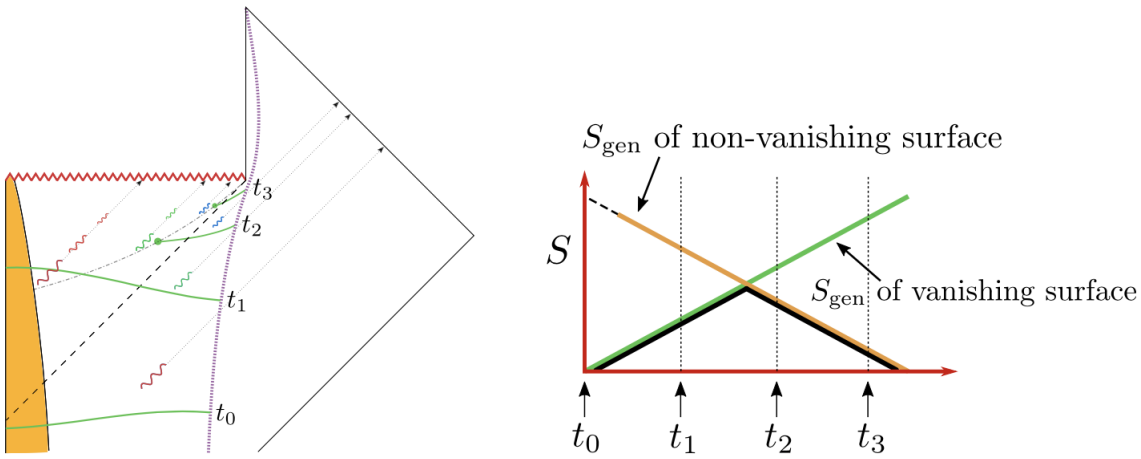

Figure 4.5: Left: A vanishing surface eventually transitions into a non-vanishing one as the black hole evaporates. Right: The Page curve (shown in black) is recovered by taking the minimum of the two cases. (Image credit: [5, Fig. 13])

4.2.1 Islands

So we saw how quantum extremal surfaces and the application of (4.1) leads us to obtain the Page curve. But we assumed that Σ_X was connected. To go further, we can consider the case when Σ_X is disconnected. This would increase first term in (4.1), i.e. the boundary area, so to ensure that the entropy is still minimised, we must correspondingly decrease the S_{sc} term. This is possible if there exists regions far away from any entangled matter, and in fact this is the situation with Hawking radiation which is entangled with fields in the black hole interior. So we can decrease S_{sc} by adding a region representing the black hole interior to the formula.

Disconnected regions like these are called 'islands', and the modified formula is given by

$$S(X) = \min_X \left\{ \text{ext}_X \left[\frac{\text{Area}(X)}{4G_N} + S_{\text{sc}}(\Sigma_{\text{rad}} \cup \Sigma_{\text{island}}) \right] \right\}, \tag{4.2}$$

where the area term now represents that of the island and we are now extremising with respect to the island [5, p. 13-14]. The setup is illustrated in Figure 4.6.

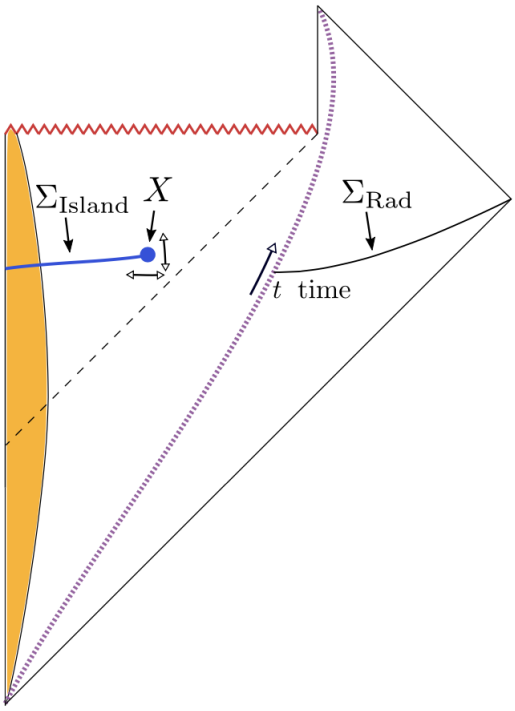

Figure 4.6: The semiclassical entropy is now calculated on the union of two regions: the island Σ_{island} and Σ_{rad}. (Image credit: [5, Fig. 14])

To use (4.2), we first find the entropy of the region from the cutoff surface to infinity. This region then represents Σ_{rad} in the formula. We then include the entropy of Σ_{island}. Just like before, we can have the case of a vanishing island. Then the semiclassical entropy only has a contribution from Σ_{rad} since the area term (which is that of the island) is zero. Σ_{rad} includes emitted Hawking radiation, so the entropy increases over time [5, p. 13], which is shown in Figure 4.7.

But a non-vanishing island appears about one scrambling time after the black hole forms. The island changes its position depending on the time on the cutoff surface [5, p. 14]. Now in this non-vanishing case, the term $S_{\text{sc}}(\Sigma_{\text{rad}} \cup \Sigma_{\text{island}})$ is close to zero since the ingoing Hawking

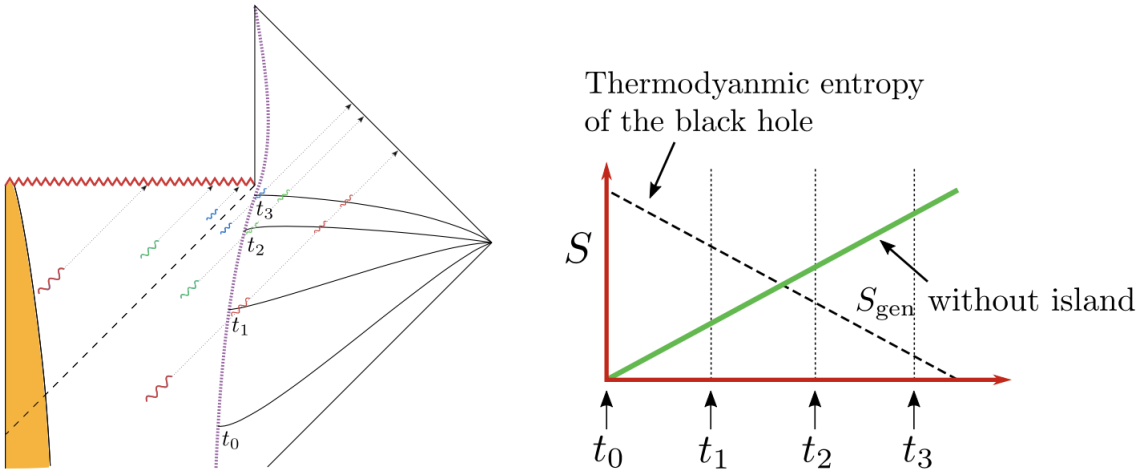

Figure 4.7: In the vanishing island case, the area term vanishes so entropy increases over time due to the emission of Hawking radiation. (Image credit: [5, Fig. 15])

radiation is combined with the outgoing radiation and therefore turns what was before a mixed state into a pure one. This means that the area term dominates, so the entropy follows the profile shown in Figure 4.8.

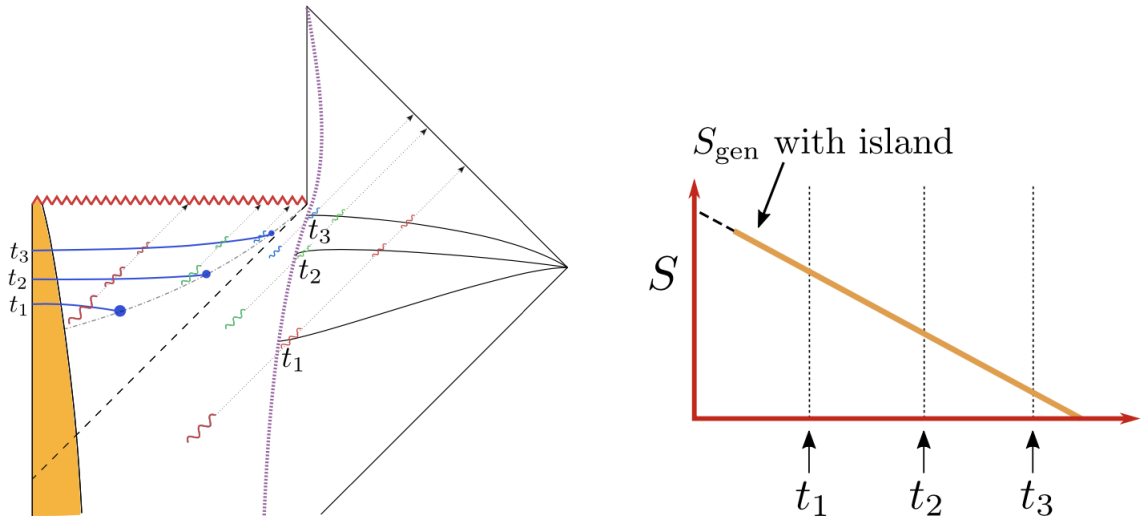

Figure 4.8: Left: A non-vanishing island appears sometime after the black hole is formed. Right: This case gives a decreasing entropy over time. (Image credit: [5, Fig. 16])

As before, the fine-grained entropy is given by the minimum of the two cases (vanishing and non-vanishing). This then leads to the Page curve in a similar fashion to the case with quantum extremal surfaces, as we see in Figure 4.9.

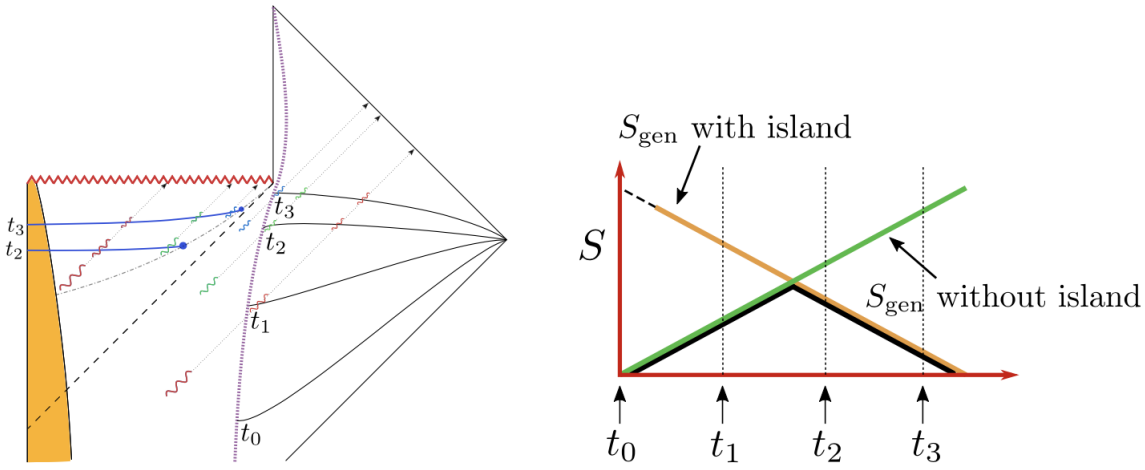

Figure 4.9: Left: The vanishing island case eventually transitions into the non-vanishing case. Right: The Page curve (shown in black) is recovered by always taking the minimum of the two cases. (Image credit: [5, Fig. 17])

4.2.2 Further work

To summarise, in this section we showed how to apply the methods in Chapter 3 to a a black hole to recover the Page curve. This was able to be achieved through considering quantum extremal surfaces. We then generalised this procedure by introducing the concept of islands.

We shall not delve too much deeper in this review, but we can go further with what's known as 'entanglement wedges'. To understand them, let us consider some quantum extremal surface. The entanglement wedge is then the region in the Penrose diagram that is causally associated with that quantum extremal surface, i.e. it is the 'causal diamond' of that quantum extremal surface [5, p. 15]. The concept of entanglement wedges were used in solving a paradox pointed out by John Wheeler in [16] which he called 'bags of gold', but that is beyond the scope of this review. We shouldn't also neglect to mention the concept of replica wormholes, which justifies including the interior when calculating the fine-grained entropy using the island formula. This was done using something called the 'replica trick' [17].

Although much progress has been made in ways to obtain the Page curve, it should be noted that many questions remain. One thing in particular that isn't understood well is the use of a cutoff surface, which played an important role in calculating the entropy in both the cases examined in this chapter. The case when the cutoff surface is the boundary of some AdS space

is well understood, but other questions remain open [5, p. 19-20].

Chapter 5

Summary and Discussion

The aim of this review was to examine the Page curve and recent developments to methods in recovering it. We began this review with introducing the essential physics of black holes and entropy that pertained to the black hole information paradox and the Page curve. We then outlined the information paradox using the nice slice argument, and then discussed what the effect of small corrections would have on the validity of the argument.

The next chapter saw a gentle introduction to the AdS/CFT correspondence, where we examined both aspects of the duality. We then explored how aspects of AdS/CFT can provide some insight on the information paradox. The main takeaway is that unitarity is preserved in black hole evaporation within its framework, although it does not tell us how. We also introduced the Ryu-Takayanagi formula as well as a formula for generalised entropy. Computing the latter formula required us to introduce the concept of quantum extremal surfaces.

Chapter 4 was devoted to the Page curve, where we applied the generalised entropy formula in the previous chapter to black hole evaporation, where we found that we were able to obtain the Page curve. We then generalised the formula to include the possibility of islands, which also lead to the Page curve being reproduced. The concepts of entanglement wedges and replica wormholes were also briefly discussed.

To fully understand the Page curve and how it is reproduced goes a long way to resolving the

information paradox. With even more progress, it is hoped that the paradox nears its end.

Bibliography

[1] S.W. Hawking, 1975. Particle creation by black holes. Commun. Math. Phys. 43 (3), 199-220. doi:10.1007/BF02345020

[2] A. Almheiri, D. Marolf, J. Polchinski, D. Stanford & J. Sully, 2013. An apologia for firewalls. J. Higher Energy Phys., 09 (018). doi:10.1007/JHEP09(2013)018

[3] S. Raju, 2022. Lessons from the information paradox. Phys. Rep., 943. doi:10.1016/j.physrep.2021.10.001

[4] R.M. Wald, 1984. General relativity. Chicago, University of Chicago Press.

[5] A. Almheiri, T. Hartman, J. Maldacena, E. Shaghoulian & A. Tajdini, 2021. The entropy of Hawking radiation. Reviews of modern physics, 93 (3). doi:10.1103/RevModPhys.93.035002

[6] M.A. Nielsen & I.L. Chuang, 2010. Quantum computation and quantum information. 10th anniversary ed., Cambridge University Press.

[7] S.D. Mathur, 2009. The information paradox: a pedagogical introduction. Class. Quantum Gravity, 26 (22). doi:10.1088/0264-9381/26/22/224001

[8] S.B. Giddings & J. Perkins, (2022) Quantum evolution of the Hawking state for black holes. arXiv:2204.13126.

[9] J. M. Maldacena, 1998. The Large N limit of superconformal field theories and supergravity. Adv. Theor. Math. Phys. 2, 231. doi:10.1063/1.59653

[10] J. M. Maldacena, 2011. The gauge/gravity duality. arXiv:1106.6073

[11] G. 't Hooft, 1993. Dimensional reduction in quantum gravity. arXiv:gr-qc/9310026

[12] L. Susskind, 1995. The world as a hologram. J. Math. Phys., 36 (11). doi:10.1063/1.531249

[13] D. Harlow, 2016. Jerusalem lectures on black holes and quantum information. Rev. Mod. Phys., 88 (1). doi:10.1103/RevModPhys.88.015002

[14] S. Ryu and T. Takayanagi, Holographic Derivation of Entanglement Entropy from the anti–de Sitter Space/Conformal Field Theory Correspondence. Phys. Rev. Lett., 96 (18). doi:10.1103/PhysRevLett.96.181602

[15] A.C. Wall, 2014. Maximin Surfaces, and the Strong Subadditivity of the Covariant Holographic Entanglement Entropy. Class. Quantum Gravity, 31 (22). doi:10.1088/0264-9381/31/22/225007

[16] J.A. Wheeler, 1964. Geometrodynamics and the issue of the final state, in Relativity, groups and topology, vol. 317.

[17] G. Penington, S.H. Shenker, D. Stanford & Z. Yang, 2022. Replica wormholes and the black hole interior. J. Higher Energy Phys., 3, (1-87). doi:10.1007/JHEP03(2022)205